

## NONLINEAR DYNAMICS OF TWO-DIMENSIONAL FLOWS: BIFURCATION, CHAOS AND TURBULENCE

T. KAMBE AND Y. KAMANAKA

Department of Physics, University of Tokyo  
Hongo, Bunkyo-ku, Tokyo 113, Japan

Two dimensional motions of a viscous incompressible fluid are investigated on the aspects of nonlinear dynamics. Equation for the vorticity gradient suggests that its dynamics in an inviscid fluid is different at points of different signs of a quantity defined in terms of the second derivatives of the streamfunction (related to the gaussian curvature). This property divides the flow domain into two regions: hyperbolic and elliptic regions for the time evolution. Turbulent cascade of the vorticity gradient spectrum is studied in a hyperbolic straining field, based on an exact analytical model.

A series of numerical simulations of the Navier-Stokes equation has been performed in order to investigate bifurcations from steady state to chaos in the two-dimensional flows with periodic boundary conditions under a certain forcing to the vorticity field. By examining the frequency spectra of the enstrophy, we have found the following sequence of transitions of the state as the viscosity decreases: steady  $\rightarrow$  simply periodic  $\rightarrow$  doubly periodic  $\rightarrow$  triply periodic  $\rightarrow$  doubly periodic (with phase locking)  $\rightarrow$  non-periodic (temporally chaotic) motion.

### 1. Introduction

Two-dimensional motions of a viscous incompressible fluid present various interesting aspects of nonlinear dynamics. This note consists of two parts. The first part of the analyses is based on the fact that the equation for the divorticity (defined<sup>2</sup> by *rotation* of the vorticity vector) is similar to the vorticity equation in the three-dimensional motion.<sup>1,3,4</sup> (The divorticity equation is equivalent to the equation for the vorticity gradient, as is evident from the definition given below.) We consider the dynamics of the divorticity and the cascade property of the divorticity layers in an irrotational field. In the direct numerical simulation of two-dimensional turbulence<sup>4,5,6</sup>, it is shown that isolated coherent vortices coexist with actively cascading turbulence, and that the rates of cascade, i.e. spectrum evolution through scale transfer, is controlled (suppressed) by the coherent vortices. In considering the cascade, it is convenient to introduce the gaussian curvature  $K$

of a hypothetical surface of the streamfunction  $z = \psi(x, y)$  in the space  $(x, y, z)$  because local dynamics are different at points of different signs of the curvature in the inviscid motions.<sup>1,4,6</sup> The flow domain is divided into two regions depending on the sign of  $K$ : hyperbolic (negative  $K$ ) and elliptic (positive  $K$ ) regions for the time evolution. To illustrate this property, three simple examples are given. Any irrotational motion is shown to have negative  $K$ , therefore it is hyperbolic. An analysis of the cascade of the divorticity in a superimposed irrotational (*i.e.* hyperbolic) straining field is presented in the section 2.2.

Owing to the advanced computers, two-dimensional fluid motions are becoming an object of detailed analyses. In the second part (§3), we consider bifurcation of the motions of a viscous incompressible fluid in a bounded domain (in a torus  $T^2$ ). The fluid motions are simulated numerically by the pseudo-spectral method in a square with periodic boundary conditions under a certain forcing. Response of the fluid system to the forcing at various values of the kinematic viscosity  $\nu$  has been investigated. Hopf bifurcations from steady state to singly periodic and further to quasi-periodic states are observed as the viscosity is decreased. It is remarkable that quadruply periodic state has not been observed in the present numerical simulations (in the range of the viscosity examined), instead temporally chaotic motions have been found. This analysis may be compared with the calculation of the flows in a cubic space.<sup>7</sup>

## 2. Dynamics of divorticity layer and cascade

### 2.1 Straining of divorticity layers and gaussian curvature of the streamfunction

In two-dimensional flows of an incompressible viscous fluid, the vorticity  $\omega(x, y, t)$  is governed by the equation,

$$\omega_t + u\omega_x + v\omega_y = \nu\nabla^2\omega , \quad (1)$$

in the  $(x, y)$  cartesian coordinates, where  $(u, v)$  are the velocity components and  $\nu$  the kinematic viscosity. By using the streamfunction  $\psi(x, y, t)$ , the velocity and vorticity are expressed as

$$u = \psi_y , \quad v = -\psi_x , \quad \omega = -\nabla^2\psi , \quad (2)$$

$$u\omega_x + v\omega_y = \partial(\omega, \psi)/\partial(x, y) . \quad (3)$$

In order to obtain an equation analogous to the vorticity equation in the 3D motion, it is convenient to use three-dimensional representation of the velocity  $v = (u, v, 0)$  and introduce the divorticity defined by

$$\eta = \nabla \times v = (\omega_y, -\omega_x, 0) = -\nabla^2v , \quad (4)$$

where  $\omega = (0, 0, \omega) = \nabla \times v$ . The following vector identity is readily shown:

$$\eta \times v = (v \cdot \nabla) \omega .$$

Thus the equation (1) is converted to the 3D form:

$$\omega_t + \eta \times v = \nu \nabla^2 \omega . \quad (5)$$

Taking the curl of this equation, one readily obtains

$$\eta_t + (v \cdot \nabla) \eta = (\eta \cdot \nabla) v + \nu \nabla^2 \eta \quad (6)$$

since  $\nabla \cdot v = 0$  and  $\nabla \cdot \eta = 0$ , where the first term on the right hand side represents stretching of the fluid element in the direction of the vector  $\eta$ .

It is interesting to compare the equations (5) and (6) with the corresponding ones in 3D motions, that is, the Navier-Stokes equation and the vorticity equation:

$$v_t + \omega \times v = \nu \nabla^2 v - \nabla \left( \frac{p}{\rho_0} + \frac{v^2}{2} \right), \quad \nabla \cdot v = 0 , \quad (7)$$

and

$$\omega_t + (v \cdot \nabla) \omega = (\omega \cdot \nabla) v + \nu \nabla^2 \omega . \quad (8)$$

In the two-dimensional fluid motion, the process of the vortex stretching is absent in the equation (1) or (5). However, if we consider the divorticity equation (6), there exists, in deed, stretching of the  $\eta$ -lines, corresponding to the stretching of vortex-lines in 3D motion described by (8).<sup>3</sup>

In an inviscid fluid ( $\nu = 0$ ), the dynamics of the divorticity  $\eta$  is simply given by

$$\frac{D}{Dt} \eta = A \eta , \quad \eta = \begin{pmatrix} \omega_y \\ -\omega_x \end{pmatrix} \quad (9)$$

where  $D/Dt = \partial/\partial t + v \cdot \nabla$  is the material derivative and the matrix  $A$  is

$$A = \begin{pmatrix} \partial_x u & \partial_y u \\ \partial_x v & \partial_y v \end{pmatrix} = \begin{pmatrix} \psi_{xy} & \psi_{yy} \\ -\psi_{xx} & -\psi_{xy} \end{pmatrix} , \quad (10)$$

which represents straining action of the fluid motion.<sup>1</sup> The equation of a passive fluid line-element  $\delta s$  has the same form:

$$\frac{D}{Dt} \delta s = A \delta s , \quad \delta s = \begin{pmatrix} \delta x \\ \delta y \end{pmatrix} \quad (11)$$

since the motion of a fluid particle  $(x(t), y(t))$  is given by  $\dot{x} = \psi_y$ ,  $\dot{y} = -\psi_x$ .<sup>8</sup> Difference between (9) and (11) lies in that the vector  $\eta$  is related to the velocity field  $v$  by  $\eta = -\nabla^2 v$ , whereas  $\delta s$  is passively carried with the fluid motion.

The eigenvalue  $\lambda$  of the matrix  $A$  satisfies

$$\lambda^2 = (\psi_{xy}^2 - \psi_{xx}\psi_{yy}) \equiv B , \quad (12)$$

therefore  $\lambda = \sqrt{B}$  or  $-\sqrt{B}$ . Denoting the corresponding eigenvector as  $\eta_\lambda$ , we have

$$\frac{D}{Dt} \eta_\lambda = \lambda \eta_\lambda \quad (13)$$

If  $B > 0$ , the two eigenvalues are real with opposite signs. In this case the dynamical evolution of  $\eta$ , following the particle motion, is hyperbolic. That is, the local (and instantaneous) effect of the straining, with respect to the particle motion, is exponentially growing or decreasing, depending on the eigen-directions. If  $B < 0$ , the eigenvalues are pure imaginary, hence the motion will be elliptic. That is, the  $\eta$  evolution is locally rotational with respect to the particle motion. In 3D turbulence, the vortex stretching is considered to be responsible for the turbulent cascade. In 2D flows, the cascade will be associated to the stretching of the divorticity as considered above. This implies that cascade process occurs in the hyperbolic regions.

Concerning the expression of  $B$  in (12) in terms of the streamfunction  $\psi(x, y)$ , it is suggestive to observe that the gaussian curvature  $K$  of the hypothetical surface  $z = \psi(x, y)$  in the  $(x, y, z)$  space is

$$K = -\frac{B}{(1 + \psi_x^2 + \psi_y^2)^2} = -\frac{\psi_{xy}^2 - \psi_{xx}\psi_{yy}}{(1 + \psi_x^2 + \psi_y^2)^2} . \quad (14)$$

Thus in the domain of negative curvature  $K$  (therefore, positive  $B$ ), the eigenvalues are real and the motion is hyperbolic, while in the domain of positive  $K$ , the eigenvalues are pure imaginary and the motion is elliptic.<sup>1</sup> In the hyperbolic region of negative curvature, the divorticity is stretched as the line element in the direction  $\eta$  is stretched. Now we consider three typical examples.

(a) The following streamfunction

$$\psi(x, y) = \sin x \sin y \quad (15)$$

represents *periodic* vortex cells. This is an exact solution of the equation (1) for  $\nu = 0$ . This is because we have  $\partial_t \omega = 0$  and  $\partial(\omega, \psi)/\partial(x, y) = 0$  since  $\omega = -\partial^2 \psi = 2\psi$ . It is readily shown that

$$B = \psi_{xy}^2 - \psi_{xx}\psi_{yy} = \cos(x - y) \cos(x + y) .$$

Thus the flow field is divided into periodic cells of the hyperbolic (H) and elliptic (E) regions (*Figure 1*). The cascade by the straining motion is expected in the H-regions.

(b) In the *irrotational* flows, the gaussian curvature  $K$  is always non-positive since

$$\omega = -(\psi_{xx} + \psi_{yy}) = 0 ,$$

and therefore we have

$$B = \psi_{xy}^2 + \psi_{xx}^2 .$$

Thus the dynamical motion of  $\eta$  is hyperbolic, except the points at  $B = 0$ .

(c) A *Rankin vortex* is defined by

$$\omega(r) = 2(r < 1), \quad 0(r > 1)$$

where  $r = (x^2 + y^2)^{1/2}$  is the radial coordinates. The corresponding streamfunction is

$$\psi(r) = -\frac{1}{2}r^2(r < 1), \quad -\log r - \frac{1}{2},$$

which gives the value  $B$  as

$$B = -1(r < 1), \quad r^{-4}(r > 1).$$

The azimuthal velocity  $v_\theta (= -\psi_r)$  (only nonzero component) is proportional to  $r$  in the inner core and decays like  $r^{-1}$  in the outer irrotational skirt (*Figure 2*). It is remarkable that the  $B$ -value takes a positive maximum just at the outside of the core, therefore a substantial hyperbolic-straining occurs at the periphery and outside of the core.

## 2.2 An exact solution representing cascade

An exact analysis can be made for a special but fairly general form of the streamfunction. Suppose that the streamfunction  $\Psi$  takes the form,

$$\Psi = axy + \psi(y, t) \tag{16}$$

where the initial form  $\psi(y, 0)$  is an arbitrary function of  $y$ , and  $a$  is assumed to be a positive constant. The first term  $axy$  represents an irrotational flow, its velocity field being  $\mathbf{v}_s = (ax, -ay)$ , while the second term represents vorticity layers since the vorticity and divorticity are given by

$$\omega(y, t) = -\psi_{yy}, \quad \eta = \omega_y = -\psi_{yyy}$$

where  $\omega = (0, 0, \omega)$  and  $\eta = (\eta, 0, 0)$ . Therefore the dynamics of hyperbolic straining of the divorticity layers can be considered by this model. The governing equations are

$$\omega_t - ay\omega_y = \nu\omega_{yy} \tag{17}$$

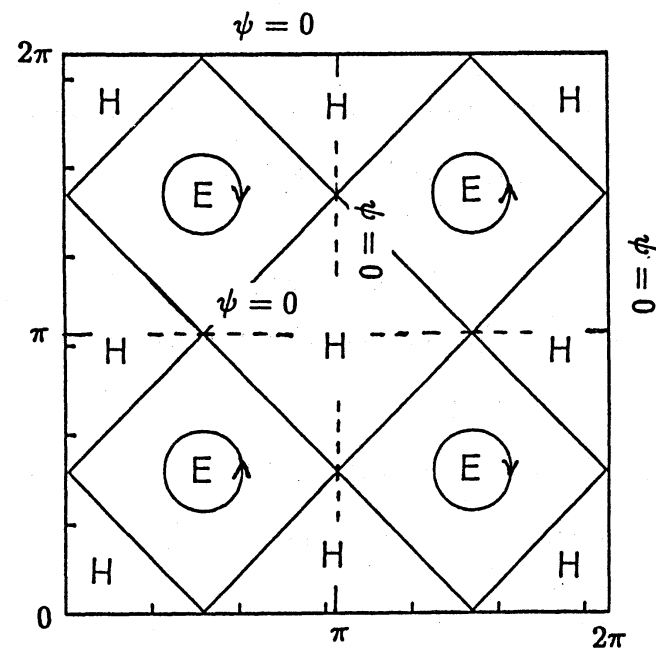


Figure 1. Hyperbolic (H) and elliptic (E) regions of the periodic vortex cells.

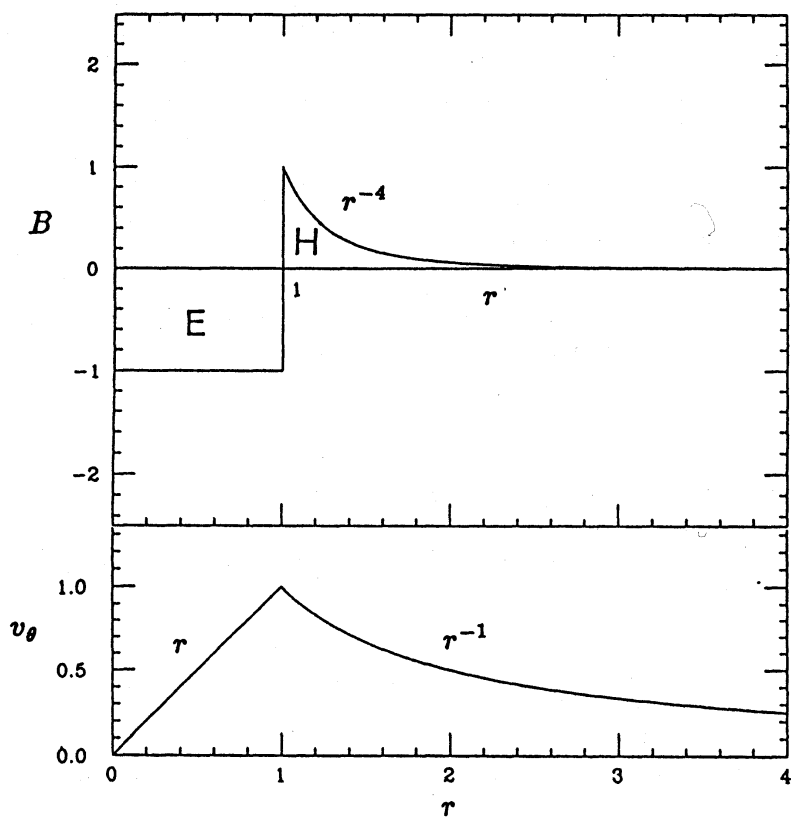


Figure 2. The values  $B$  and  $v_\theta$  of the Rankin vortex.

for the vorticity (from (1)) and

$$\eta_t - a y \eta_y = a \eta + \nu \eta_{yy} \quad (18)$$

for the divorticity.

The equation (18) represents the motion of the divorticity layers  $\eta(y, t)$  under the combined action of viscous diffusion ( $\nu \eta_{yy}$ ), stretching ( $a\eta$ ) and convective straining ( $-ay\eta_y$ ). This type of equation is considered by Kambe<sup>8</sup> to study the motion of a shear layer in a three dimensional straining field  $(ax, by, cz)$  with the total velocity field given by  $(ax + V(y, t), by, cz)$ , where  $a, b$  and  $c$  may be time-dependent and satisfy the solenoidal condition of the velocity,  $a + b + c = 0$ .

Introducing new variables defined by

$$\xi = A(t)y, \quad \tau(t) = \int_0^t A^2(t') dt', \quad F(\xi, \tau) = \eta(y, t)/A(t), \quad (19)$$

where

$$A(t) = e^{at},$$

one can transform the equations (17) and (18) into the diffusion equations,

$$\omega_\tau = \nu \omega_{\xi\xi}, \quad F_\tau = \nu F_{\xi\xi} \quad (20)$$

respectively.

For a general initial condition of the form  $\omega(y, 0) = \omega_0(y)$ , the vorticity  $\omega(y, t)$  is written as

$$\omega(y, t) = \frac{1}{(4\pi\nu\tau(t))^{1/2}} \int_{-\infty}^{\infty} \omega_0(y') \exp\left[-\frac{(Ay - y')^2}{4\nu\tau}\right] dy'. \quad (21)$$

Similarly, replacing  $\omega_0$  by the initial divorticity  $\eta_0(y) = \eta(y, 0)$  in (21), the right hand side gives the solution for the normalized divorticity  $F(\xi, \tau) = \eta(y, t)/A(t)$ .

The Fourier spectrum of the divorticity is given by

$$\hat{\eta}(k, t) = \exp\left[-\nu k^2 \frac{\tau(t)}{A^2(t)}\right] \hat{\eta}_0\left(\frac{k}{A(t)}\right), \quad (22)$$

where  $\hat{\eta}_0(k)$  is the initial Fourier spectrum. This states that the straining field  $v_s = (ax, -ay)$  produces transfer of the initial spectrum  $\hat{\eta}_0(k_0)$  to a higher wave number  $k = k_0 A(t)$  with the amplitude diminished by the viscous effect represented by the exponential factor  $\exp[-\nu k^2 \tau(t)/A^2(t)]$ . It is interesting to find that, as  $t$  becomes sufficiently large,  $\tau(t)/A^2(t)$  tends to the constant  $1/2a$ . Thus we have

$$\hat{\eta} \rightarrow \exp(-\nu k^2/2a) \hat{\eta}_0(k/A(t)), \quad \text{as } t \rightarrow \infty. \quad (23)$$

This implies a viscous cut-off wave number  $k_d$  may be given by

$$k_d = (2a/\nu)^{1/2}. \quad (24)$$

Another combination of the independent variables  $(t, \xi)$  reduces the equation (18) to  $\eta_t = a\eta$  for the inviscid case  $\nu = 0$ . This gives the exponentially growing solution  $\eta = e^{at}\eta_0(\xi)$ .

For the divorticity  $\eta(y, t)$  governed by the equation (18), one may define the correlation function,

$$P(\zeta, t) = \langle \eta(y, t) \eta(y + \zeta, t) \rangle$$

and its Fourier representation,

$$P(\zeta, t) = \int_{-\infty}^{\infty} \hat{P}(k, t) e^{ik\zeta} dk ,$$

where  $\langle \rangle$  means an ensemble average.

In this ensemble, the  $y$ -origin at which the divorticity layers converge is assumed to be uniformly distributed along the  $y$  axis, allowing  $P$  to be independent of  $y$ . The Fourier transform  $\hat{P}(k, t)$  gives the spectrum of the palinstrophy  $\langle \eta^2(y, t) \rangle$ .

For the convenience of later consideration, we define the mean kinetic energy  $E$ , enstrophy  $Q$  and palinstrophy  $P$  by

$$\begin{aligned} E(t) &= \frac{1}{2} \langle |v|^2 \rangle = \frac{1}{2} \langle (u^2 + v^2) \rangle = \int \hat{E}(k, t) dk , \\ Q(t) &= \frac{1}{2} \langle \omega^2 \rangle = \int \hat{Q}(k, t) dk , \\ P(t) &= \frac{1}{2} \langle |\eta|^2 \rangle = \frac{1}{2} \langle (\omega_y^2 + \omega_x^2) \rangle = \int \hat{P}(k, t) dk , \end{aligned} \quad (25)$$

where  $\hat{E}(k, t)$  is the energy spectrum,  $\hat{Q}(k, t) = k^2 \hat{E}(k, t)$  the enstrophy spectrum and  $\hat{P}(k, t) = k^4 \hat{E}(k, t)$  the palinstrophy spectrum.

The equation of  $P(\zeta, t)$  can be derived from (18) as

$$P_t - a\zeta P_\zeta = 2aP + 2\nu P_{\zeta\zeta} , \quad (26)$$

leading to the equation for the Fourier transform ,

$$\hat{P}_t + a \frac{\partial}{\partial k} (k \hat{P}) = 2a\hat{P} - 2\nu k^2 \hat{P} . \quad (27)$$

Suppose that the ensemble average is stationary, so that  $\hat{P}_t = 0$ . Then we have

$$a \frac{d}{dk} (k \hat{P}) = 2a\hat{P} - 2\nu k^2 \hat{P} , \quad (28)$$

which is readily solved, yielding

$$\hat{P}(k) = Ck \exp\left(-\frac{\nu k^2}{a}\right) .$$

In an inertial range in which the inequality  $k^2 \ll k_d^2$  holds, we obtain  $\hat{P}(k) \sim C k$ . This leads to the enstrophy spectrum  $\hat{Q}(k) \sim k^{-1}$  and the energy spectrum  $E(k) \sim k^{-3}$  of the enstrophy cascade studied by Batchelor<sup>11</sup>, Kraichnan<sup>9</sup> and Leith<sup>10</sup>.

In the numerical simulations of two dimensional decaying turbulence,<sup>4,6</sup> it is known that there remain coherent vortices in the final period of decay. The analysis of the energy spectrum due to Benzi et al.<sup>6</sup> shows that the spectrum of the part restricted to the coherent vortices is described by the power law  $E(k) \sim k^{-4.3}$ , <sup>0</sup> whereas the spectrum in the remaining part where the hyperbolic straining of the divorticity is expected to occur is described by the law  $E(k) \sim k^{-3}$ . The latter spectrum coincides with that of enstrophy cascade discussed above.

This suggests the view that dynamical development of the two-dimensional flow is different in the regions of elliptic and hyperbolic straining.

### 3. Numerical analysis of bifurcations of viscous incompressible flows

A series of numerical simulations of the Navier-Stokes equation has been performed to investigate bifurcations from steady state to chaotic motion in two-dimensional viscous incompressible flows with a periodic boundary condition as the viscosity  $\nu$  is lowered from a sufficiently large value to attain a steady state.<sup>12</sup> For all the values of  $\nu$ , the computation started from a common initial (motionless) state, and final states obtained by the computation for different  $\nu$  are investigated.

#### 3.1 Method of numerical analysis

Two-dimensional motion of a viscous fluid is described by the vorticity equation (1), which is rewritten in the form:

$$\frac{\partial}{\partial t} \omega = \frac{\partial^2}{\partial x \partial y} S - \left( \frac{\partial^2}{\partial x^2} - \frac{\partial^2}{\partial y^2} \right) T + \nu \left( \frac{\partial^2}{\partial x^2} + \frac{\partial^2}{\partial y^2} \right) \omega , \quad (29)$$

where  $S(x, t) = u^2 - v^2$  and  $T(x, t) = u v$ , with  $x = (x, y)$ , are introduced for convenience of the numerical computation.

This equation is solved numerically for prescribed initial values. The velocity field is assumed to be periodic with a period of  $2\pi$  in both  $x$  and  $y$ -directions. We expand  $v(x, t)$ ,  $\omega(x, t)$ ,  $S(x, t)$  and  $T(x, t)$  in the Fourier series, e.g. as

$$v(x, t) = \sum_{\mathbf{k}} \hat{v}(\mathbf{k}, t) \exp[i\mathbf{k} \cdot \mathbf{x}] , \quad \omega(x, t) = \sum_{\mathbf{k}} \hat{\omega}(\mathbf{k}, t) \exp[i\mathbf{k} \cdot \mathbf{x}] , \dots \quad (30)$$

---

<sup>0</sup> During the Symposium, Dr. Marie Farge commented that the spectrum restricted to the coherent vortices depends on the initial condition and therefore the energy spectrum of two-dimensional turbulence is not considered to be universal.

together with the condition of reality  $\hat{v}^*(k, t) = \hat{v}(-k, t)$ , where  $k = (k_x, k_y)$  is the wave number vector whose components are integers and the symbol \* denotes the complex conjugate. The summations with respect to  $k$  are taken over all integer components between  $-N/2$  and  $N/2$  ( $N$  being a given even integer).

Fourier transform of the equation (29) is

$$\frac{d}{dt}\hat{\omega}(k, t) = -k_x k_y \hat{S}(k, t) + (k_x^2 - k_y^2)\hat{T}(k, t) - \nu k^2 \hat{\omega}(k, t), \quad (31)$$

( $k^2 = k_x^2 + k_y^2$ ), which is supplemented with the Fourier transforms of the vorticity  $\omega = v_x - u_y$  and the solenoidal condition  $u_x + v_y = 0$ . The latter two relations in combination lead to

$$v(k, t) = i(k_y, -k_x) \frac{1}{k^2} \hat{\omega}(k, t).$$

These equations are solved under prescribed initial conditions.

#### *Numerical scheme and initial conditions*

In carrying out the numerical computation, the Fourier expansions (30) are restricted to the summation over  $-N/2 \leq k_x, k_y \leq N/2$ . Once we know all the Fourier components  $\hat{\omega}(k, T)$  at a time  $t$ , the time derivative  $d\hat{\omega}/dt$  is obtained by calculating the three terms on the right hand side of (31). The first and second terms are estimated by the pseudo-spectral method<sup>13,14</sup>, whereas the third term is trivial. The aliasing errors in the calculation of the nonlinear terms are eliminated by truncating the Fourier modes at the wave number  $K = N/3$ .

Initial values of  $\hat{\omega}$  at  $t = 0$  are specified as

$$\begin{aligned} \hat{\omega}(1, 0) &= (0.148270369158839464 + 0.645628691483143568 i)/4 \\ \hat{\omega}(1, 1) &= (0.935990691629399776 - 0.576029181218477607 i)/4 \\ \hat{\omega}(0, 1) &= (-0.784594893146804333 + 0.923589110235304952 i)/4 \\ \hat{\omega}(1, -1) &= (-0.327462077122592509 + 0.230159521544059587 i)/4 \end{aligned}$$

which were randomly generated by the computer. The condition of reality immediately specifies the values of  $\hat{\omega}(-1, 0)$ ,  $\hat{\omega}(-1, -1)$ ,  $\hat{\omega}(0, -1)$  and  $\hat{\omega}(-1, 1)$ . The other components are set as  $\hat{\omega} = 0$ . The initial contour of the vorticity  $\omega(x, 0)$  is shown in figure 3.

In the present study we have taken the condition that the eight lowest modes  $\hat{\omega}(k, t)$  for  $k = (\pm 1, 0)$ ,  $(0, \pm 1)$ ,  $(\pm 1, \pm 1)$  are fixed throughout the time. This means that the external forcing is imposed only at the lowest modes and the enstrophy injected at those modes cascades to higher wavenumber modes, and that the inverse energy cascade (to lower modes) will be inhibited in this situation.

The time marching of (31) was carried out by the fourth-order Runge-Kutta scheme. The parameters  $\nu$ ,  $N$  and  $\Delta t$  used in the computation are shown in Table 1.

Table 1. The parameters used in the computation

	$N$	$\Delta t$
$\nu \geq 0.0009$	128	0.02
$\nu \leq 0.0009$	256	0.01

### 3.2 Temporal behaviors of the enstrophy

Numerical computation has been performed for various values of viscosity:  $\nu = 0.0027 \sim 0.0006$ . As a result of time evolution, the fluid system approaches a state of different behaviors depending on the  $\nu$ -value : *steady state* (S), *simply periodic state* (SP), doubly-periodic (*quasi-periodic*) state (QP<sub>2</sub>), triply-periodic state (QP<sub>3</sub>), QP<sub>2</sub> with phase-locking (QP<sub>2</sub>\*), or *non-periodic state* (NP).

Steady state is attained as a final state at the viscosity  $\nu$  ranging from 0.0027 to 0.0023. As the viscosity decreases further, the system evolves to a time-dependent state. Examining the temporal behavior of the enstrophy  $Q(t)$ , defined by using the Fourier components,

$$Q(t) = \frac{1}{2} \sum_{|k_x|, |k_y| \leq K} |\hat{\omega}(k, t)|^2 , \quad (32)$$

we have found the following sequence of transitions to non-periodic (chaotic) state as the viscosity decreases: S  $\Rightarrow$  SP  $\Rightarrow$  QP<sub>2</sub>  $\Rightarrow$  QP<sub>3</sub>  $\Rightarrow$  QP<sub>2</sub>\*  $\Rightarrow$  NP . The types of motion which were realized finally by the numerical computation (with a fixed viscosity) are summarized in Table 2.

In Figure 4a, the temporal behavior of the enstrophy at the viscosity  $\nu = 0.0020$  is shown. It oscillates regularly in time and the amplitude of the oscillation is kept constant. To examine the state more closely, we have made Fourier transformation of the time series of the enstrophy  $Q$ . The Fourier coefficient is given by

$$\hat{Q}(\sigma) = \sum_{m=1}^M Q(T + m\Delta t) \exp(i\sigma m\Delta t) .$$

The total time span taken in the transform  $M\Delta t$  is about 1550 and the spectral interval  $\Delta\sigma = 2\pi/M\Delta t$  is  $4.793 \times 10^{-3}$ . The initial time  $T + \Delta t$  for the transform is chosen at the times after the initial transient motion ceased.

In Figure 5a, the frequency power spectrum  $|\hat{Q}(\sigma)|^2$  for  $\nu = 0.0020$  is plotted. Three peaks are observed in the figure. By detailed examination of the inverse of the spectrum ( so-called *parabola fitting*), it is confirmed that they have one fundamental frequency  $\sigma_1$  and the other two are its second and third harmonics. The second frequency coincides with  $2\sigma_1$  within an error of order  $10^{-5}$ , while the third is different from  $3\sigma_1$  by  $8 \times 10^{-4}$ . This is, however, much smaller than the frequency interval  $\Delta\sigma = 47.9 \times 10^{-4}$ . From these evidences, this motion is considered to be simply periodic.

Table 2. Types of motion obtained for the viscosity  $\nu$ 

state	$\nu$	state	$\nu$
S	0.0027	0.0026	0.00152
	0.0025	0.0024	0.0015
	0.0023		0.0014
SP	0.0022	0.0021	0.0013
	0.0020	0.0019	0.00125
	0.0018	0.0017	(phase locking) 0.0012 0.0011
	0.0016		0.0010 0.0009
QP <sub>2</sub>	0.00158	0.00156	NP 0.0008 0.0007
	0.00154		0.0006

The behavior of the enstrophy at  $\nu = 0.00156$  is shown in *Figure 4b*. Its frequency power spectrum has several distinct peaks (*Figure 5b*). We have checked that all of these frequencies are expressed by sums and differences of two fundamental frequencies  $\sigma_1$  and  $\sigma_2$ . Thus it is found that this motion is doubly periodic (*quasi-periodic* when the two frequencies are incommensurable).

*Figures 4c* and *5c* show the temporal behavior and its power spectrum of the enstrophy at  $\nu = 0.0014$  respectively. The spectrum has a lot of peaks. Especially noted that a new peak is observed at about  $\sigma = 0.075$ . This is the third frequency  $\sigma_3$  which cannot be expressed by a sum or difference of simple multiples of  $\sigma_1$  and  $\sigma_2$ . We have checked that all the frequencies of the peaks can be expressed as linear combinations of the three fundamental frequencies  $\sigma_1$ ,  $\sigma_2$  and  $\sigma_3$ . Therefore the motion is a triply periodic state.

In *Figure 4d* the temporal behavior of the enstrophy at  $\nu = 0.0013$  is plotted and in *Figure 5d* its power spectrum is shown. In this case, three frequencies  $\sigma_1$ ,  $\sigma_2$  and  $\sigma_3$  are not incommensurable, but it is found that the relation  $2\sigma_2 = \sigma_1 + \sigma_3$  holds. This relation continues to exist for the values of viscosity  $\nu = 0.00125$ ,  $0.0012$ ,  $0.0011$ .

At  $\nu = 0.0010$ , at first a triply periodic motion seems to be realized from  $t = 500$  to  $3200$ , but finally it turns into an irregular behavior (*Figures 4e* and *5e*).

At  $\nu = 0.0006$ , the behavior appears non-periodic (*Figure 4f*). The spectrum has too many peaks (*Figure 5f*). Counting the number of the peak spectral components in the frequency domain  $0 \leq \sigma \leq 2$  it is found that it amounts to nearly a half of the total number of the spectral components. Existence of such many peaks supports the assertion that the spectrum in this case may be continuous and therefore the motion is non-periodic. The vorticity contour at the final instant of the computation is shown in *Figure 6* for this type of non-periodic motion with the lowest value of the viscosity  $\nu = 0.0006$  examined in the present study.

The behavior of the energy or the palinstrophy are similar to that of the enstrophy.

#### 4. Summary and discussion

We have considered two-dimensional incompressible motions of a viscous fluid from two different approaches. The analysis in the first part is based on the property that, when the viscosity effect is weak, the flow field is divided into two regions, hyperbolic and elliptic regions, and the dynamics are different in each region. An exact analytical model is presented and it is applied to the analysis of turbulent cascade of the divorticity in a superimposed hyperbolic straining field.

In the second part a series of numerical simulations is presented, in which the flow field is represented by Fourier modes and the motion is driven by the imposed condition (*i.e.* forcing) that eight lowest Fourier modes are kept constant at all times. The fluid system starts from motionless initial state. When the viscosity is larger than (or equal to) 0.0023, the flow field attains a steady state. When  $\nu$  is decreased, the total enstrophy (or energy) begins to oscillate at a single frequency and does not tend to a final steady state. This may be interpreted as *Hopf bifurcation* of the fluid system having a large number of degrees of freedom. For even smaller values of the viscosity, the system bifurcates to a motion of double or triple periodicities in time (as a result of sequence of Hopf bifurcations), to a state of phase-locking, and further to a non-periodic or chaotic state.

We have obtained the state of three-frequency quasi-periodicity, however a quadruply periodic motion has not been observed. A triply periodic motion is considered to be structurally unstable to a  $C^2$  perturbation, while a  $C^\infty$  perturbation destabilizes a motion of  $n$ -frequency quasi-periodicity for  $n \geq 4$ .<sup>15,16</sup> Since the present analysis is a numerical study, one cannot state a definite answer. So that, the observed triply periodic motion may evolve to a chaotic state in the long run as was the case for  $\nu = 0.0010$ , or it may be such a weak chaotic state with dominant three frequencies that we cannot distinguish it from a triply periodic motion. However we cannot exclude the possibility also that a triply periodic motion does exist as Grebogi et al.<sup>17</sup> pointed out. Anyway it is remarkable that the Ruelle-Takens scenario has been observed in the present numerical simulation of viscous incompressible flows on the torus  $T^2$  and also in the three-dimensional simulation on  $T^3$  by Kida et al.<sup>7</sup>

## REFERENCES

1. J. Weiss, The dynamics of enstrophy transfer in two-dimensional hydrodynamics. *LJI-TN-81-121* (1981), La Jolla Inst., La Jolla, California.
2. S. Kida, *J. Phys. Soc. Jpn.* **54**(8) (1985) 2840.
3. M.E. Brachet, M. Meneguzzi, H. Politano and P.L. Sulem, *J. Fluid Mech.* **194** (1988) 333.
4. J.C. McWilliams, *J. Fluid Mech.* **146** (1984) 21.
5. J.C. McWilliams, *Phys. Fl.* **A 2**(4) (1990) 547.
6. R. Benzi, S. Patarnello and P. Santangelo, *J. Phys. A* **21** (1988) 1221.
7. S. Kida, K. Ohkitani and M. Yamada, *Physica D* **37** (1989) 116.
8. T. Kambe, Some dissipation mechanisms in vortex systems. in *Turbulence and Chaotic Phenomena in Fluids*, ed. T. Tatsumi, (Elsevier Sci. Pub., Amsterdam, 1984), 239.
9. R. Kraichnan, *Phys. Fl.* **10**, (1967) 1417.
10. C.E. Leith, *Phys. Fl.* **11**, (1968) 671.
11. G.K. Batchelor, *Phys. Fl. Supplement II*, **12**, (1969) II-233.
12. Y. Kamanaka, Numerical study of bifurcations in two-dimensional viscous incompressible flows. Master thesis (Dept. of Physics, University of Tokyo, 1989).
13. S.A. Orszag, *Stud. Appl. Math.* **50**, (1971) 293.
14. C. Canuto, M.Y. Hussaini, A. Quarteroni and T.A. Zang, *Spectral Methods in Fluid Dynamics*, (Springer, New York, 1988).
15. D. Ruelle and F. Takens, *Commun. Math. Phys.* **20**, (1971) 167.
16. S. Newhouse, D. Ruelle and F. Takens, *Commun. Math. Phys.* **64**, (1978) 35.
17. C. Grebogi, E. Ott and J. York, *Phys. Rev. Lett.* **51** (1983) 339.

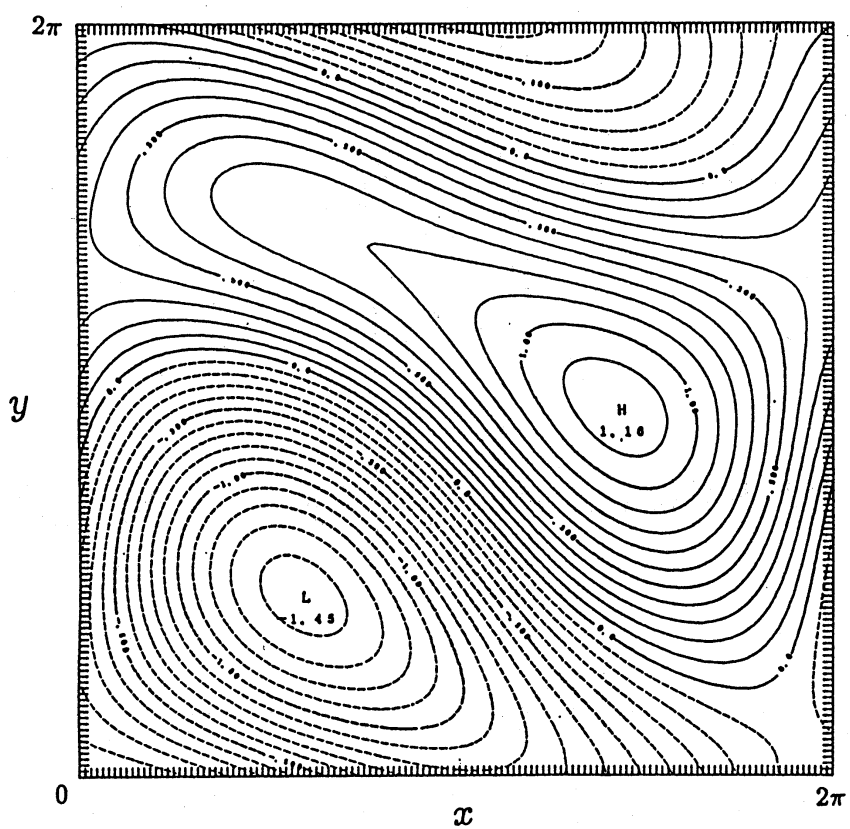


Figure 3. Initial contours of the vorticity field  $\omega(x, 0)$ . Positive or negative extremum is denoted by the symbol H or L, respectively.

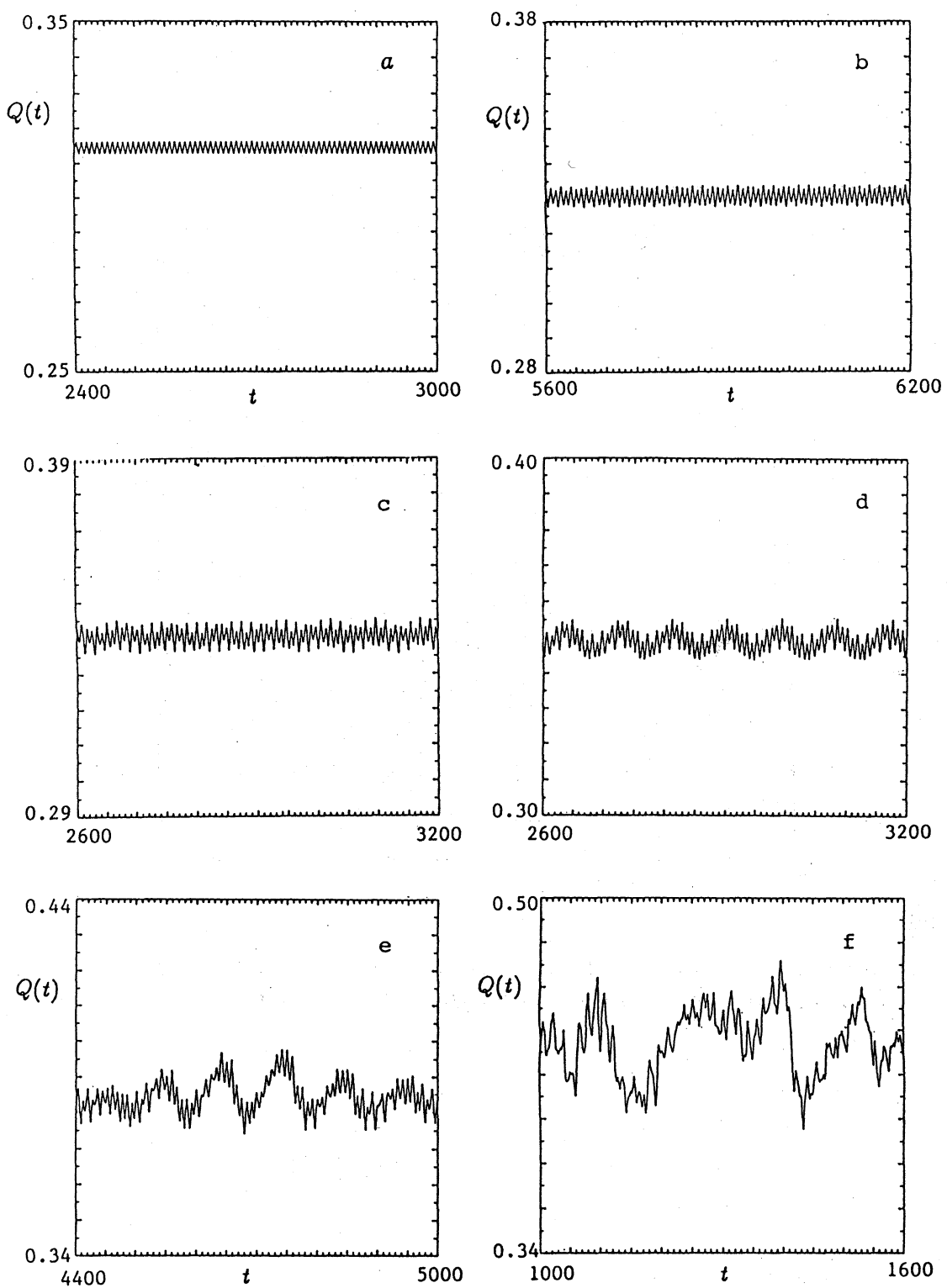


Figure 4. Temporal behaviors of the enstrophy  $Q(t)$  for the viscosity  $\nu$ :  
 (a) 0.0020, (b) 0.00156, (c) 0.0014, (d) 0.0013,  
 (e) 0.0010 and (f) 0.0006.

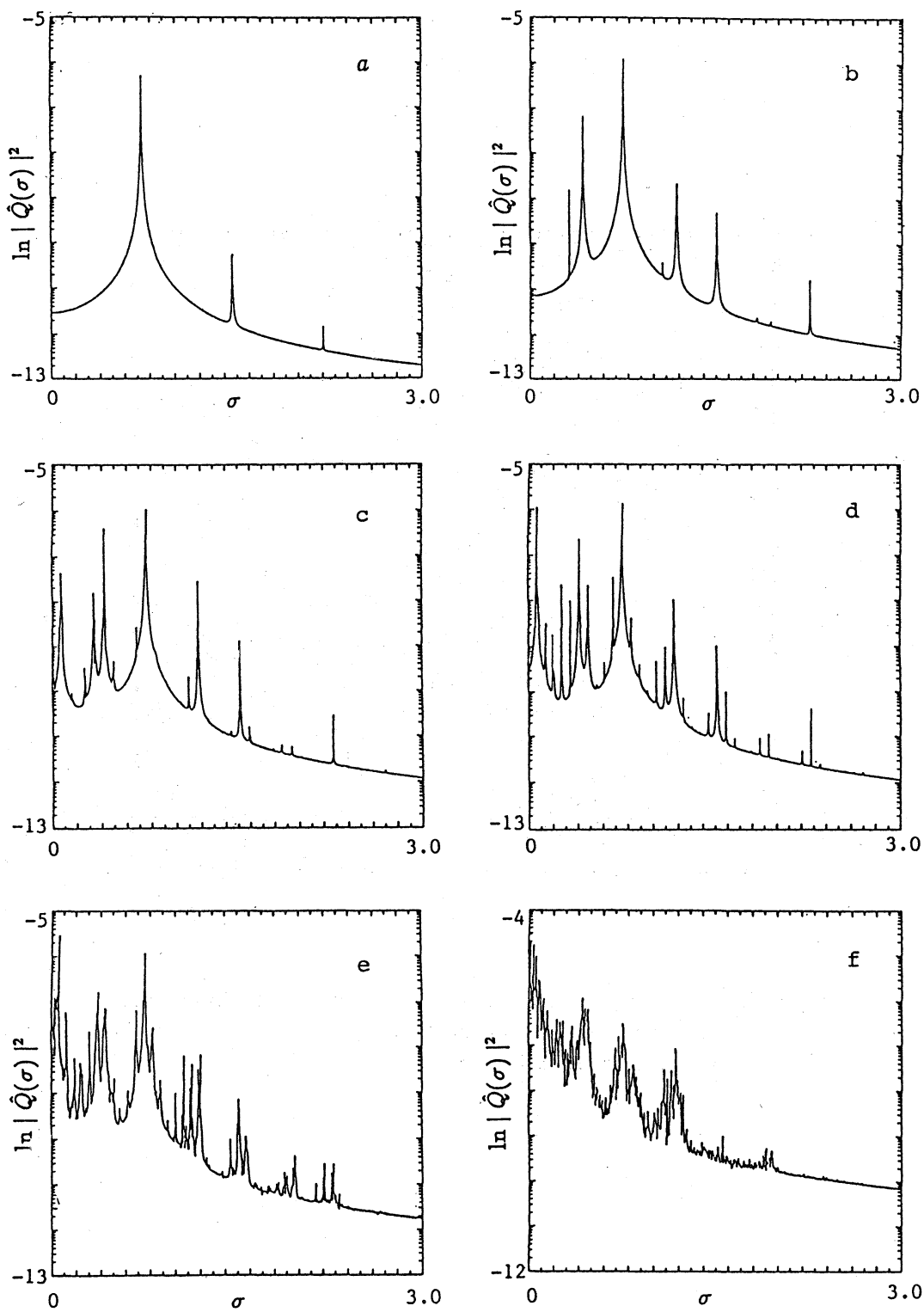


Figure 5. Frequency power spectrum  $\ln |\hat{Q}(\sigma)|^2$  for the cases corresponding to Figure 4.

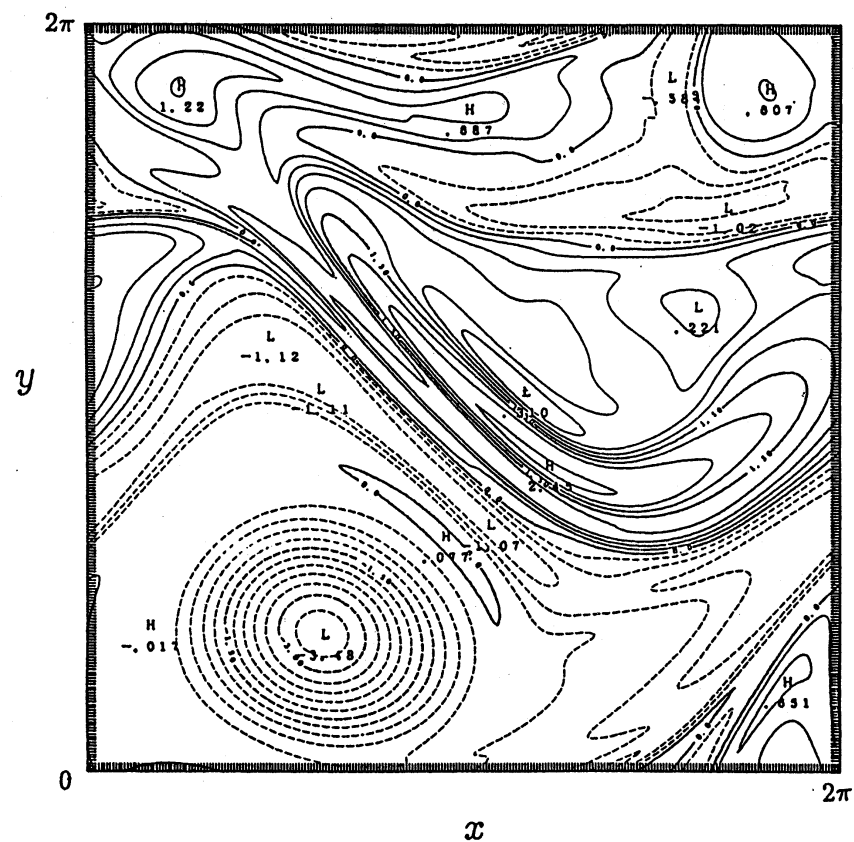


Figure 6. The vorticity contours at the final instant of computation for the lowest value of the viscosity  $\nu = 0.0006$ . The symbols H and L are as in Figure 3.